CHAPTER 1

Size and Properties of Particles

1.1 Introduction

The flow characteristics of solid particles in a gas–solid suspension vary significantly with the geometric and material properties of the particle. The geometric properties of particles include their size, size distribution, and shape. Particles in a gas–solid flow of practical interest are usually of nonspherical or irregular shapes and polydispersed sizes. The geometric properties of particles affect the particle flow behavior through an interaction with the gas medium as exhibited by the drag force, the distribution of the boundary layer on the particle surface, and the generation and dissipation of wake vortices. The material properties of particles include such characteristics as physical adsorption, elastic and plastic deformation, ductile and brittle fracturing, solid electrification, magnetization, heat conduction and thermal radiation, and optical transmission. The material properties affect the long- and short-range interparticle forces, and particle attrition and erosion behavior in gas–solid flows. The geometric and material properties of particles also represent the basic parameters affecting the flow regimes in gas–solid systems such as fluidized beds.

In this chapter, the basic definitions of the equivalent diameter for an individual particle of irregular shape and its corresponding particle sizing techniques are presented. Typical density functions characterizing the particle size distribution for polydispersed particle systems are introduced. Several formulae expressing the particle size averaging methods are given. Basic characteristics of various material properties are illustrated.

1.2 Particle Size and Sizing Methods

The particle size affects the dynamic behavior of a gas–solid flow [Dallavalle, 1948]. An illustration of the relative magnitudes of particle sizes in various multiphase systems is given in Fig. 1.1 [Soo, 1990]. It is seen in this figure that the typical range of particle sizes of interest to gas–solid flows is roughly from 1 μm to 10 cm. The particle shape affects the flowability of powders, their packing, and the covering power of pigments. Qualitative definitions for particle shapes are given in Table 1.1. The shape of particles is commonly expressed in terms of shape factors and shape coefficients [Allen, 1990].

Particles used in practice for gas–solid flows are usually nonspherical and polydispersed. For a nonspherical particle, several equivalent diameters, which are usually based on equivalences either in geometric parameters (*e.g.*, volume) or in flow dynamic characteristics (*e.g.*, terminal velocity), are defined. Thus, for a given nonspherical particle, more than one equivalent diameter can be defined, as exemplified by the particle shown in Fig. 1.2, in which three different equivalent diameters are defined for the given nonspherical particle. The selection of a desired definition is often based on the specific process application intended.

Table 1.1. *Definitions of Particle Shape*

Acicular	needle-shaped
Angular	sharp-edged or having roughly polyhedral shape
Crystalline	freely developed in a fluid medium of geometric shape
Dendritic	having a branched crystalline shape
Fibrous	regularly or irregularly thread-like
Flaky	plate-like
Granular	having approximately an equidimensional irregular shape
Irregular	lacking any symmetry
Modular	having rounded, irregular shape
Spherical	global shape

Source: T. Allen's *Particle Size Measurements*, Chapman & Hall, 1990.

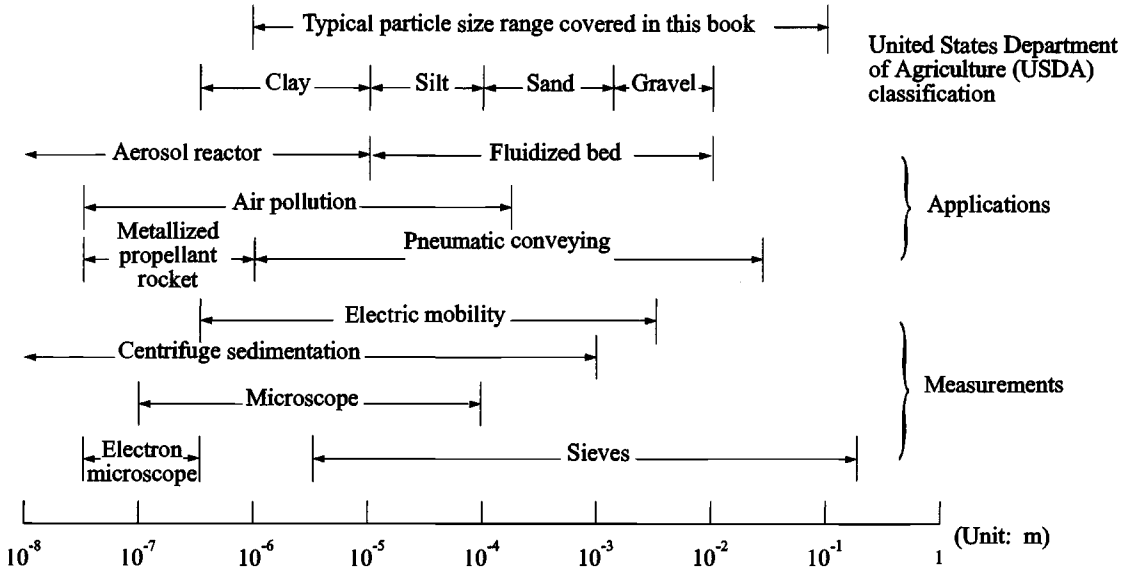

Figure 1.1. Magnitudes of particle sizes in gas–solid systems (after Soo, 1990).

1.2.1 *Equivalent Diameters of a Nonspherical Particle*

An equivalent diameter of a particle is usually defined in relation to a specific sizing method developed on the basis of a certain equivalency criterion. Several equivalent diameters of a spherical particle commonly employed are discussed in the following sections.

1.2.1.1 *Sieve Diameter*

A sieve diameter is defined as the width of the minimum square aperture through which the particle will pass. A common sizing device associated with this definition is a series of sieves with square woven meshes. Two sieve standards, *i.e.*, Tyler Standard and American

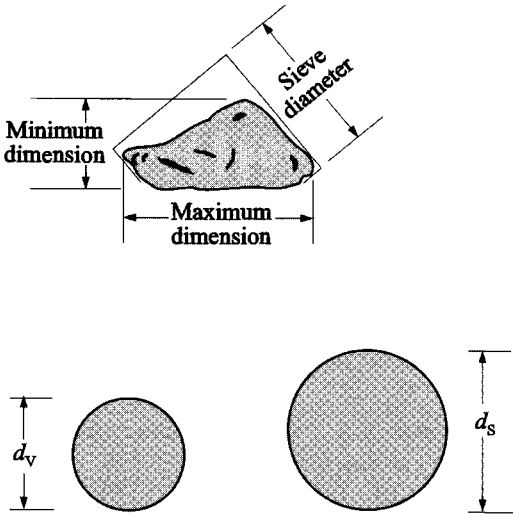

Figure 1.2. Schematic illustration of multidimensions of a particle and its equivalent volume diameter, surface diameter, and sieve diameter.

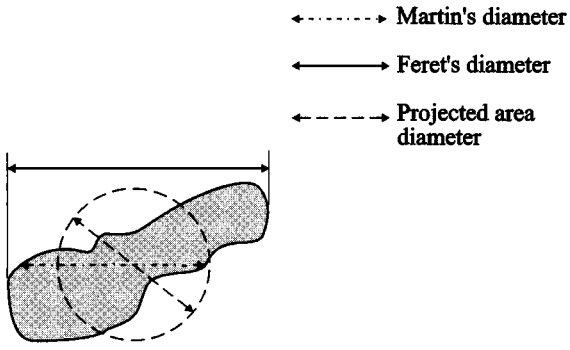

Figure 1.3. Schematic illustration of different particle diameters based on 2-D projected image.

Society for Testing and Materials (ASTM) Standard, are widely used; they are introduced in §1.2.2.1.

1.2.1.2 *Martin's Diameter, Feret's Diameter, and Projected Area Diameter*

Martin's diameter, Feret's diameter, and projected area diameter are three diameters defined on the basis of the projected image of a single particle. Specifically, Martin's diameter is defined as the averaged cord length of a particle which equally divides the projected area. Feret's diameter is the averaged distance between pairs of parallel tangents to the projected outline of the particle. The projected area diameter is the diameter of a sphere having the same projected area as the particle. These diameters are schematically represented in Fig. 1.3. The projected area diameter of a particle d_A can be related to the particle projected

area A by

$$d_A = \left(\frac{4A}{\pi}\right)^{1/2} \tag{1.1}$$

Martin's diameter and Feret's diameter of a particle depend on the particle orientation under which the measurement is made. Thus, obtaining a statistically significant measurement for these diameters requires a large number of randomly sampled particles which are measured in an arbitrarily fixed orientation. Since Martin's diameter, Feret's diameter, and projected area diameter are based on the two-dimensional image of the particles, they are generally used in optical and electron microscopy. The principles of microscopy as a sizing method are discussed in §1.2.2.2.

1.2.1.3 *Surface Diameter, Volume Diameter, and Sauter's Diameter*

The surface diameter, d_S, volume diameter, d_V, and Sauter's diameter, d_{32}, are defined such that each of them reflects a three-dimensional geometric characteristic of an individual particle. A surface diameter is given as the diameter of a sphere having the same surface area as the particle, which is expressed by

$$d_S = \sqrt{\frac{S}{\pi}} \tag{1.2}$$

where S is the particle surface area. A volume diameter is the diameter of a sphere having the same volume as the particle, which is defined by

$$d_V = \left(\frac{6V}{\pi}\right)^{1/3} \tag{1.3}$$

where V is the particle volume. The Sauter's diameter or surface-volume diameter is defined as the diameter of a sphere having the same ratio of external surface to volume as the particle, which is given by

$$d_{32} = \frac{6V}{S} = \frac{d_V^3}{d_S^2} \tag{1.4}$$

The concept of the surface diameter may be mostly used in the field of adsorption and reaction engineering, where the equivalent surface exposure area is important. The determination of the surface area depends on the method of measurements; for example, permeametry can give a much lower area than does gas adsorption. The latter often includes the contribution of pore surface area, which is accessible to the gas molecules. The determination of particle surface area by gas adsorption is given in §1.2.2.4. The fundamentals of gas adsorption are further covered in §1.4.1.

The volume diameter of a particle may be useful in applications where equivalent volume is of primary interest, such as in the estimation of solids holdup in a fluidized bed or in the calculation of buoyancy forces of the particles. The volume of a particle can be determined by using the weighing method. Sauter's diameter is widely used in the field of reacting gas–solid flows such as in studies of pulverized coal combustion, where the specific surface area is of most interest.

1.2.1.4 *Dynamic Diameter*

The dynamic response of a particle in gas–solid flows may be characterized by the settling or terminal velocity at which the drag force balances the gravitational force. The dynamic diameter is thus defined as the diameter of a sphere having the same density and the same terminal velocity as the particle in a fluid of the same density and viscosity. This definition leads to a mathematical expression of the dynamic diameter of a particle in a Newtonian fluid as

$$V(\rho_p - \rho)g = C_D \frac{\pi}{8} \frac{\mu^2}{\rho} \mathrm{Re}_t^2$$
$$d_t = \frac{\mathrm{Re}_t \mu}{\rho U_{pt}} \tag{1.5}$$

where Re_t is the particle Reynolds number at the terminal velocity; C_D is the drag coefficient, which is a function of Re_t; μ denotes the viscosity of the fluid; ρ and ρ_p represent the densities of the fluid and the particle, respectively; U_{pt} is the particle terminal velocity; g is the gravitational acceleration; and d_t is the equivalent dynamic diameter.

The relationship between C_D and Re_t for a sphere is given by Fig. 1.4 [Schlichting, 1979]. Mathematically, it can be expressed by

$$C_D = \frac{24}{\mathrm{Re}_t} \qquad \mathrm{Re}_t < 2$$
$$C_D = \frac{18.5}{\mathrm{Re}_t^{0.6}} \qquad 2 < \mathrm{Re}_t < 500 \tag{1.6}$$
$$C_D = 0.44 \qquad 500 < \mathrm{Re}_t < 2 \times 10^5$$

The three correlations in Eq. (1.6), in order from top to bottom, are known as Stokes's, Allen's, and Newton's equations, respectively. Combining these equations with Eq. (1.5),

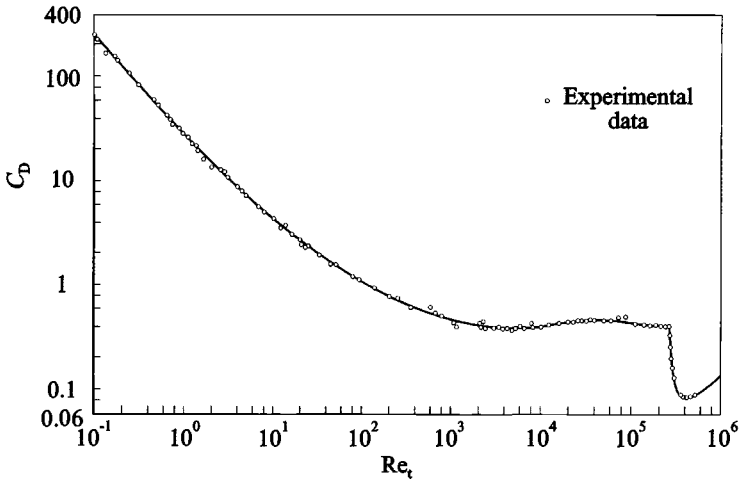

Figure 1.4. Drag coefficient for spheres as a function of Re_t (from Schlichting, 1979).

the terminal velocity of a sphere is related to its diameter by

$$\begin{aligned} U_{pt} &= \frac{d_t^2(\rho_p - \rho)g}{18\mu} && \mathrm{Re}_t < 2 \\ U_{pt}^{1.4} &= 0.072\frac{d_t^{1.6}(\rho_p - \rho)g}{\rho^{0.4}\mu^{0.6}} && 2 < \mathrm{Re}_t < 500 \\ U_{pt}^2 &= 3.03\frac{d_t(\rho_p - \rho)g}{\rho} && 500 < \mathrm{Re}_t < 2 \times 10^5 \end{aligned} \tag{1.7}$$

It is noted that in the laminar flow region, the particle moves in random orientation; however, outside this region it orients itself so as to give the maximum resistance to the motion. Thus, the dynamic diameter of an irregular-shaped particle in the intermediate region may be greater than that in the laminar flow region.

Example 1.1 One of the applications of using Stokes's law to determine the particle size is the Sedigraph particle analyzer. Table E1.1 shows the relationship between the cumulative weight percentage of particles and the corresponding particle terminal velocities for a powder sample. The densities of the particle and the dispersing liquid are 2,200 and 745 kg/m^3, respectively. The liquid viscosity is 1.156×10^{-3} kg/m·s. Find out the relationship of the mass fraction distribution to the equivalent dynamic diameter.

Table E1.1. *Cumulative Weight Percentage Versus Terminal Velocity*

U_{pt} (m/s)	Cumulative wt%	U_{pt} (m/s)	Cumulative wt%
4.4×10^{-3}	99.9	1.1×10^{-5}	65.6
2.5×10^{-3}	99.3	6.2×10^{-6}	47.2
1.7×10^{-3}	99.2	2.7×10^{-6}	21.2
6.2×10^{-4}	98.5	6.9×10^{-7}	1.2
1.5×10^{-4}	96.0	4.4×10^{-7}	1.0
6.9×10^{-5}	93.0	2.5×10^{-7}	0.8
4.4×10^{-5}	90.1	1.7×10^{-7}	0.4
2.5×10^{-5}	83.5	1.1×10^{-7}	0.2
1.7×10^{-5}	76.8	2.7×10^{-8}	0.1

Solution Rearranging Eq. (1.7), the dynamic diameter for $\mathrm{Re}_t < 2$ is given as

$$d_t = \sqrt{\frac{18\mu}{(\rho_p - \rho)g}U_{pt}} \tag{E1.1}$$

which yields the dynamic diameter from the given terminal velocity, as given in Table E1.2. The weight fraction within the range of two neighboring dynamic diameters is also tabulated in Table E1.2, from which the mass distribution versus the dynamic diameter is obtained, as shown in Fig. E1.1.

Table E1.2. *Mass Fraction (wt%) Versus Dynamic Diameter*

U_{pt} (m/s)	d_t (μm)	f_M (wt%)
4.4×10^{-3}	80	0.6
2.5×10^{-3}	60	0.1
1.7×10^{-3}	50	0.7
6.2×10^{-4}	30	2.5
1.5×10^{-4}	15	3.0
6.9×10^{-5}	10	2.9
4.4×10^{-5}	8	6.6
2.5×10^{-5}	6	6.7
1.7×10^{-5}	5	11.2
1.1×10^{-5}	4	18.4
6.2×10^{-6}	3	26.0
2.7×10^{-6}	2	20.0
6.9×10^{-7}	1	0.2
4.4×10^{-7}	0.8	0.2
2.5×10^{-7}	0.6	0.4
1.7×10^{-7}	0.5	0.2
1.1×10^{-7}	0.4	0.1
2.7×10^{-8}	0.2	

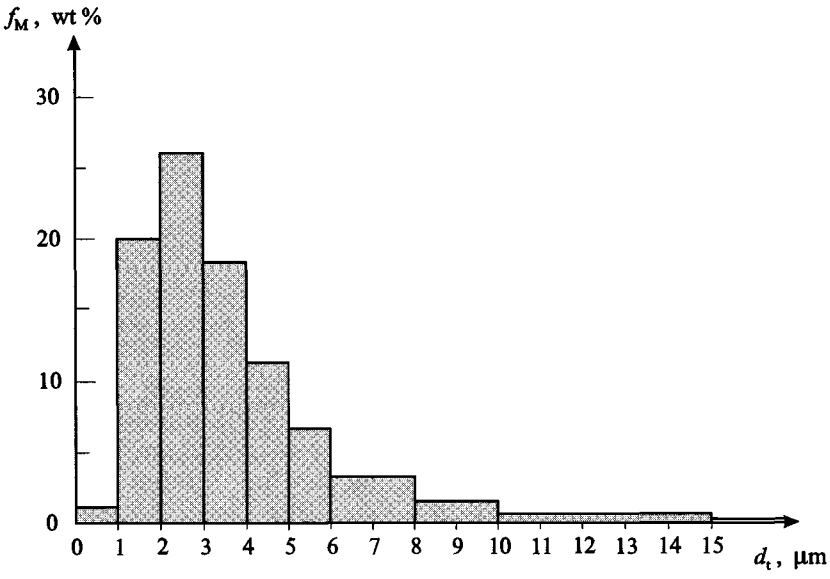

Figure E1.1. Mass fraction distribution based on data in Table E1.2.

Table 1.2. *Some Methods of Particle Size Measurement*

Method	Size range (μm)
Sieving	
Woven wire	37–5660
Electroformed	5–120
Punched plate	50–125,000
Microscopy	
Optical	0.8–150
Electron	0.001–5
Sedimentation	
Gravitational	5–100
Centrifugal	0.001–1,000
Fraunhofer diffraction	0.1–1,000
Doppler phase shift	1–10,000

1.2.2 *Particle Sizing Methods*

The sizing methods involve both classical and modern instrumentations, based on a broad spectrum of physical principles. The typical measuring systems may be classified according to their operation mechanisms, which include mechanical (sieving), optical and electronic (microscopy, laser Doppler phase shift, Fraunhofer diffraction, transmission electron miscroscopy [TEM], and scanning electron microscopy [SEM]), dynamic (sedimentation), and physical and chemical (gas adsorption) principles. The methods to be introduced later are briefly summarized in Table 1.2. A more complete list of particle sizing methods is given by Svarovsky (1990).

1.2.2.1 *Sieving*

Sieving is the simplest and most widely used technique for powder classification. This method is based only on the size of the particles and is independent of other particle properties (*e.g.*, density, optical properties, and surface roughness).

The common sieves are made of woven wire cloth and have square apertures. The sizes of the sieve openings have been standardized, and currently two different sets of standard series, the Tyler Standard and the U.S. Series ASTM Standard, are used in the United States. The mesh number of a sieve is normally defined as the number of apertures per unit area (square inch). Thus, the higher the mesh number the smaller the aperture. Typical mesh numbers, aperture sizes, and wire diameters are given for the Tyler sieves and the U.S. ASTM sieves in Table 1.3. Sieve analysis covers the approximate size range of 37 μm to 5,660 μm using standard woven wire sieves. Electroformed micromesh sieves extend the range down to 5 μm or less while punched plate sieves extend the upper limit.

It should be pointed out that longer sieving time can improve the recovery of a given particle size for a distribution; however, excessive sieving can lead to particle degradation due to attrition or mechanical wear. This effect can be especially pronounced for particles near the tail end of the size distribution. Unfortunately, neither good theories nor reliable empirical formulae are available to estimate the optimum sieving time under which a narrow error margin of the resulting size distribution can be ensured for a given sample.

Table 1.3. *Tyler Standard and U.S. ASTM Sieve Series*

	Tyler standard		U.S. series ASTM standard		
Mesh no.	Size (μm)	Wire diameter (μm)	Mesh no.	Size (μm)	Wire diameter (μm)
$3\frac{1}{2}$	5,660	1,280–1,900	$3\frac{1}{2}$	5,613	1,650
4	4,760	1,140–1,680	4	4,699	1,650
5	4,000	1,000–1,470	5	3,962	1,120
6	3,360	870–1,320	6	3,327	914
7	2,830	800–1,200	7	2,794	833
8	2,380	740–1,100	8	2,362	813
10	2,000	680–1,000	9	1,981	838
12	1,680	620–900	10	1,651	889
14	1,410	560–800	12	1,397	711
16	1,190	500–700	14	1,168	635
18	1,000	430–620	16	991	597
20	840	380–550	20	833	437
25	710	330–480	24	701	358
30	590	290–420	28	589	318
35	500	260–370	32	495	300
40	420	230–330	35	417	310
45	350	200–290	42	351	254
50	297	170–253	48	295	234
60	250	149–220	60	246	179
70	210	130–187	65	208	183
80	177	114–154	80	175	142
100	149	96–125	100	147	107
120	125	79–103	115	124	97
140	105	63–87	150	104	66
170	88	54–73	170	88	61
200	74	45–61	200	74	53
230	62	39–52	250	61	41
270	53	35–46	270	53	41
325	44	31–40	325	43	36
400	37	23–35	400	38	25

1.2.2.2 *Microscopy*

Microscopy is often referred to as an absolute method for the determination of size and size distribution of small particles because it allows direct visualization and measurements of individual particles. Three commonly used types are optical microscopy, transmission electron microscopy (TEM), and scanning electron microscopy (SEM).

The optical microscope is one of the most basic instruments for particle sizing and is applicable to a typical size range of 0.8 μm to 150 μm. The lower limit is a result of the diffraction effects on the particle image as observed in a microscope. The limit of resolution of an optical microscope can be estimated by (Yamate and Stockham, 1977)

$$\delta = \frac{1.22\lambda}{2N_A} \tag{1.8}$$

where δ is the limit of resolution; λ is the wavelength of the light; and N_A is the numerical

Table 1.4. *The Maximum Useful Magnification and the Eyepiece Required for Different Objectives*

Objective					
Magnification	Focal length (mm)	Numerical aperture	Depth of focus (μm)	Maximum useful magnification	Eyepiece required
2.5	56	0.08	50	80	30
10	16	0.25	8	250	25
20	8	0.50	2	500	25
43	4	0.66	1	660	15
97	2	1.25	0.4	1,250	10

Source: A. G. Guy's *Essentials of Materials Science*, McGraw-Hill, 1976.

aperture of the objective. As an example, for visible light of $\lambda = 4{,}500$ Å and with an objective aperture having $N_A = 1.25$, the limit of resolution of the optical microscope can be calculated from Eq. (1.8) as 0.2 μm.

An appropriate selection of the maximum useful magnification of an optical microscope for a given sample is also important. The magnification of the microscope is the product of the objective-eyepiece combination. As a rule of thumb, the maximum useful magnification for the optical microscope is 1,000 times the numerical aperture. Table 1.4 summarizes the maximum useful magnification and the eyepiece required for different objectives.

The TEM and SEM are two advanced techniques which use electron beams for direct determination of the particle size and surface area. They are usually applied to measurement of particles in a size range of 0.001 μm to 5 μm. The TEM generates an image of a particle sample on a photographic plate by means of an electron beam, through the transmissibility of the electron beam on the sample. The SEM uses a fine beam of electrons of medium energy (5–50 keV) to scan across the sample in a series of parallel tracks. These scanning electrons produce secondary electron emission, back scattered electrons, light, and X-rays which can be detected. Both the TEM and SEM are extensively used in the determination of the pore structure and surface shape and area of the particle. The SEM is considerably faster and gives more three-dimensional information than the TEM. Details about the TEM and SEM are given by Kay (1965) and Hay and Sandberg (1967), respectively.

1.2.2.3 *Sedimentation*

The sedimentation techniques utilize the dependence of the terminal velocities of particles on their size either in a gravitational field or in a centrifugal field. The lower limit of the particle sizing by the gravitational sedimentation method is about 5 μm because of the effects of convection, diffusion, and Brownian motion as well as the long settling time involved. These effects can be overcome by centrifuging the suspension, which accelerates the settling process. Centrifugal sedimentation is mostly applied to the particle size range of 0.001 μm to 1 mm.

The sedimentation methods are normally used to measure the size of particles in a liquid medium because of the relatively high viscosity effects in liquids compared to gases. The particles in a liquid may become solvated, yielding increased weight and volume of the particle. Meanwhile, the buoyant effect on the solvated particle in the surrounding medium

increases. In the determination of the overall driving force for sedimentation, these two effects are noted to cancel each other. Therefore, solvation usually has little effect on the particle sizing results when the sedimentation methods in liquids are used.

By analogy, the definition of dynamic diameter in a centrifugal field can be simply extended from Eq. (1.5) with the replacement of the gravitational acceleration, g, by the centrifugal acceleration, $\omega^2 r$, as

$$V(\rho_p - \rho)\omega^2 r = C_D \frac{\pi}{8} \frac{\mu^2}{\rho} \mathrm{Re}_t^2$$
$$d_t = \frac{\mathrm{Re}_t \mu}{\rho U_{pt}} \tag{1.9}$$

where ω is angular frequency and r is the radial distance from the center of the centrifugal field.

1.2.2.4 *Gas Adsorption*

As indicated earlier, the surface area of porous particles is an important variable in characterizing physical or chemical processes involving these particles. Porous particles commonly encountered in catalysis and reaction engineering include activated carbon, alumina, silica, and zeolites. For a given porous particle, the effective surface area is defined on the basis of the specific transport phenomenon of interest in a process system. For example, thermal radiation may be affected predominantly by the external surface area of the particle and the exposed surface area due to superficial cracks and fissures. On the other hand, for most chemical reactions and adsorption processes, the internal surface area provided by the interior pores of the particle may determine the overall rate process. A convenient classification of pores according to their width divides them into three categories: micropores, less than 20 angstrom (Å); mesopores, between 20 and 500 Å; and macropores, more than 500 Å. An exception of a large specific surface which is wholly external in nature is provided by a dispersed aerosol composed of fine particles free of cracks and indentations [Gregg and Sing, 1982].

The most common method used for the determination of surface area and pore size distribution is physical gas adsorption (also see §1.4.1). Nitrogen, krypton, and argon are some of the typically used adsorptives. The amount of gas adsorbed is generally determined by a volumetric technique. A gravimetric technique may be used if changes in the mass of the adsorbent itself need to be measured at the same time. The nature of the adsorption process and the shape of the equilibrium adsorption isotherm depend on the nature of the solid and its internal structure. The Brunauer–Emmett–Teller (BET) method is generally used for the analysis of the surface area based on monolayer coverage, and the Kelvin equation is used for calculation of pore size distribution.

It is noted that in the evaluation of the particle surface diameter and Sauter's diameter, as discussed in §1.2.1.3, only the external surface area of the particle is considered.

1.2.2.5 *Fraunhofer Diffraction*

The particle sizing technique using light scattering and diffraction possesses some advantages. It is nonintrusive and much faster than that using a mechanical means, requiring neither a conducting medium nor a large shearing force. The implementation of Mie theory

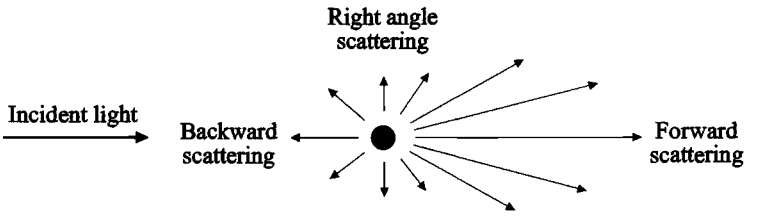

Figure 1.5. Illustration of the angular light intensity distribution of light scattered from a single particle.

with Fraunhofer diffraction and side scatter permits the measurement of particle sizes over a range of 0.1–1000 μm [Plantz, 1984].

From the Beer–Lambert law, the transmittance for a light beam through a sample of particles is given by

$$\frac{I_t}{I_i} = \exp(-nA_e l) \tag{1.10}$$

where I_t is the intensity of the transmitted beam; I_i is the intensity of the incident beam; n is the particle number concentration; A_e is the integrated cross section for extinction, which includes the effects of reflection, refraction, diffraction, and absorption; and l is the optical path length. The extinction cross section can be calculated from the Lorenz–Mie theory. A typical angular distribution of light scattered from a single particle is illustrated in Fig. 1.5. It shows that the most scattering is in the forward direction.

Although the Lorenz–Mie theory is exact, it does not lead to simple and analytical solutions relating the particle size to transmittance measurements. However, there are limiting cases where much simpler theories have been established. These limiting cases are the Rayleigh scattering for particles much smaller than the wavelength of light and the Fraunhofer diffraction for particles much larger than the wavelength of light. A criterion for discerning limiting cases is proposed by van de Hulst (1981) as

$$\begin{aligned} &\kappa < 0.3 && \text{Rayleigh scattering} \\ &\kappa \approx 1 && \text{Lorenz–Mie theory} \\ &\kappa \gg 30 && \text{Fraunhofer diffraction} \end{aligned} \tag{1.11}$$

The parameter κ is defined as

$$\kappa = \frac{2\pi d|n_i - 1|}{\lambda} \tag{1.12}$$

where n_i is the relative index of refraction of the particle.

In this book, particles larger than 1 μm are of primary interest, and thus, only the Fraunhofer diffraction method, which can account for particles larger than 2–3 μm, is discussed here. The Fraunhofer diffraction theory is derived from fundamental optical principles that are not concerned with scattering. To obtain the Fraunhofer diffraction, two basic requirements must be satisfied. First, the area of the particle or aperture must be much smaller than the product of the wavelength of light and the distance from the light source to the particle or aperture. Second, this area must also be smaller than the product

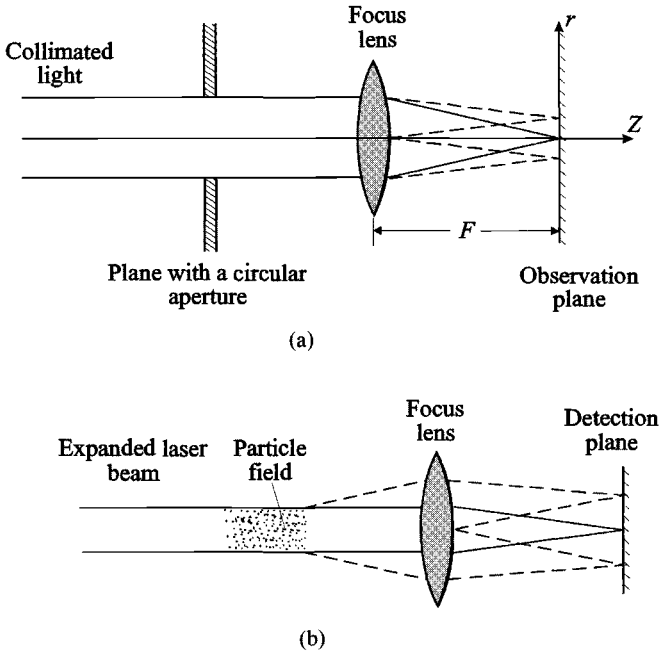

Figure 1.6. Fraunhofer diffraction system for particle size analysis: (a) Diffraction by a circular aperture; (b) Diffraction by a particle cloud.

of the wavelength and the distance from the particle or aperture to the observation plane. Therefore, Fraunhofer diffraction is known as far-field diffraction. A schematic diagram for the Fraunhofer diffraction of a single particle or aperture is illustrated in Fig. 1.6(a), whereas an optical schematic of a Fraunhofer diffraction instrument for the analysis of particle sizes in a gas–solid suspension system using a laser beam as the light source is shown in Fig. 1.6(b).

The transmittance of Fraunhofer diffraction for a circular aperture or spherical particles of diameter d can be expressed by

$$\frac{I_t}{I_i} = \left(\frac{2J_1(x)}{x}\right)^2 \tag{1.13}$$

where J_1 is the first-order spherical Bessel function and x is given by

$$x = \frac{\pi d r}{\lambda F} \tag{1.14}$$

where r is the radial distance in the observation plane as measured from the optical axis and F is the focal length of the lens. Thus, the Fraunhofer diffraction pattern for a circular aperture or spherical particles can be determined as shown in Fig. 1.7. Consequently, by measuring and analyzing the intensity distributions of the light beam over a finite area of the detector, the equivalent particle diameter can be obtained. More detailed information about the Fraunhofer diffraction method is given by Weiner (1984).

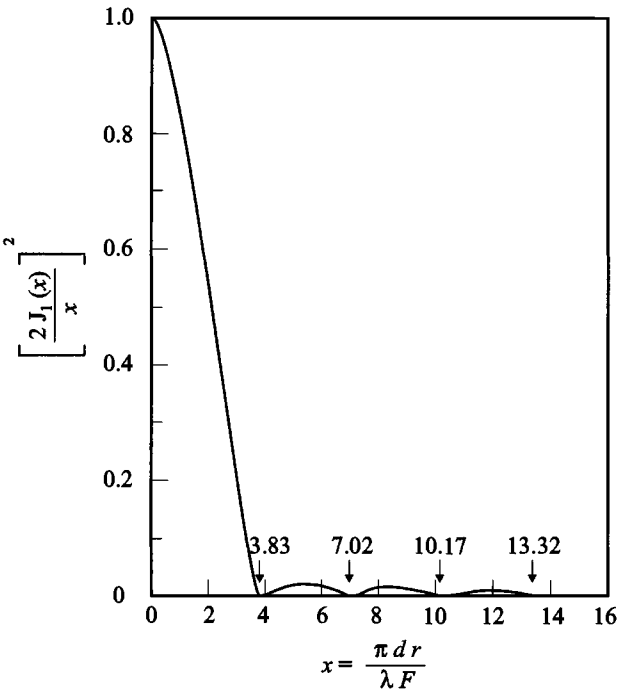

Figure 1.7. Fraunhofer diffraction pattern for circular aperture or opaque disk (from Weiner, 1984).

1.2.2.6 *Laser Doppler Phase Shift*

When a spherical particle enters the crossing volume of two laser beams, a Doppler effect occurs not only in frequency shift but also in phase shift of the scattered light. The frequency shift yields the velocity of the sphere, whereas the phase shift gives the particle size. The phase Doppler principle has been employed to measure the size and size distributions of spheres in addition to the particle velocity. The phase Doppler principle was first reported by Durst and Zaré (1975) and became a viable measurement tool one decade later [Bachalo and Houser, 1984].

The phase Doppler principle can be described as follows: When light is scattered by a small spherical particle traveling through a laser measurement volume, it yields frequency signals, which can be measured to obtain the particle velocity. This frequency is known as the Doppler shift frequency, which is identical in all spatial directions. When viewed from two separate spatial locations the scattered signals exhibit a phase shift whose magnitude depends on factors including the angle at which light is scattered to each photodetector, the index of refraction of the material of the spherical particle, and parameters such as the light wavelength and the beam intersection angle. When reflection is the dominant mode of scattering, the phase shift is independent of the index of refraction. The phase shift measured in the Doppler signal obtained from the same particle using two closely spaced photodetectors varies linearly with the particle diameter for spherical particles and hence provides a useful means for determining the spherical particle size. Evaluation of the relationship of the phase shifts from the signals received at each of the photodetector locations is complex but can be determined on the basis of Mie scattering theory [Bachalo

and Houser, 1984]. In principle, the measurement of particle size requires that the particle entering the measurement volume be spherical, and the diameters of amorphous particles cannot be measured using the phase Doppler method.

Typically, the phase Doppler method is good for the measurement of particle sizes ranging from 1 μm to 10 mm with a variation by a factor of 40 at one instrument setting. As a rule of thumb, the maximum measurable concentration is 1,000 particles per cubic millimeter (mm^3). Commercial instruments using this technique are available, *e.g.*, the phase Doppler particle analyzer (PDPA) (Aerometrics) and the Dantec particle dynamics analyzer (DPDA) (Dantec Electronics).

1.2.2.7 *Coulter Principle*

The Coulter principle underlies a method for determining particle sizes and size distributions using an electrical sensing technique. The instrument based on the Coulter principle is known as the Coulter counter. In the Coulter counter, particles are first suspended in an electrolyte and then passed through a small orifice. The particle concentration is usually so low that particles traverse the orifice one at a time. The orifice has immersed electrodes. When a particle passes through the orifice, it displaces electrolyte within the orifice, which results in a change in impedance leading to a voltage pulse with an amplitude proportional to the volume of the particle. By regulating, sizing, and number counting of the pulses, the particle size and size distributions are obtained. The typical sizing range by the Coulter counter is from 1 to 50 μm.

1.2.2.8 *Cascade Impactor*

When particles are small enough, the sedimentation method becomes inefficient as a result of the impractically long settling time. An important design using the inertial technique is known as the cascade impactor, which samples and classifies particle sizes by their inertia. A cascade impactor consists of a series of collecting plates of the particle-laden gas flow, which is gradually increased in the form of a succession of jets. Thus, deflected by inertia, the particles are collected and graded on the series collecting plates. The extent of the particle deposition on each plate depends on the impact velocity of the gas stream. The intake velocity should be low enough to prevent any damage on the collecting plates. However, it should also be high enough to ensure sufficient inertia of the particles. The most commonly used cascade impactor is the one developed by May (1945). The May cascade impactor is capable of sampling airborne particles from 0.5 to 50 μm by using four or more collecting glass discs. The particle sizing range by cascade impactors is typically from 0.1 to 100 μm.

1.3 Particle Size Distributions and Averaged Diameters

For a system of polydispersed particles, various averaged diameters may be defined according to the diversity of needs in industrial applications. An averaged diameter depends not only on the type of particle size distribution but also on the selection of a weighing factor. A particle size density function can be defined in terms of either the number of particles or the mass of particles within a given size range. The number density function is interconvertible with its corresponding mass density function. Different weighing factors with their distinct physical significance may be imposed to yield various averaged diameters for particles in a polydispersed system.

1.3.1 *Density Functions*

A number density function, $f_N(b)$, is defined so that $f_N(b)\,db$ represents the particle number fraction in a size range from b to $b + db$. Thus,

$$\frac{dN}{N_0} = f_N(b)\,db \tag{1.15}$$

where dN is the number of particles within the size range of b to $b + db$ for a total number N_0 of the sample particles. Clearly, the preceding expression leads to a normalized condition

$$\int_0^\infty f_N(b)\,db = 1 \tag{1.16}$$

Thus, over a range from d_1 to d_2, the fraction of the total sample N_0 of this size is obtained by

$$\frac{N_{12}}{N_0} = \int_{d_1}^{d_2} f_N(b)\,db \tag{1.17}$$

A particle density function can also be defined in terms of the particle mass. A mass density function, $f_M(b)$, represents the particle mass fraction in size by

$$\frac{dM}{M_0} = f_M(b)\,db \tag{1.18}$$

where dM is the mass of particles within the size range of b to $b + db$ for a total mass M_0 of the sample particles. Thus, the normalized condition for a mass density function is given by

$$\int_0^\infty f_M(b)\,db = 1 \tag{1.19}$$

and, over a range from d_1 to d_2, the fraction of the total sample M_0 of the mass is found from

$$\frac{M_{12}}{M_0} = \int_{d_1}^{d_2} f_M(b)\,db \tag{1.20}$$

It is noted that the mass of particles can be expressed in terms of the number of particles of the same size, or

$$dM = m\,dN \tag{1.21}$$

where m is the mass of a single particle of size b. For a spherical particle, m can be expressed by

$$m = \frac{\pi}{6}\rho_p b^3 \tag{1.22}$$

From Eqs. (1.15), (1.18), and (1.21), the number density function is related to the mass density function by

$$f_M(b) = \frac{N_0 m}{M_0} f_N(b) \tag{1.23}$$

The number density function is usually obtained by using microscopy or other optical means such as Fraunhofer diffraction. The mass density function can be acquired by use of sieving or other methods which can easily weigh the sample of particles within a given size range.

1.3.2 *Typical Distributions*

In the applications of gas–solid flows, there are three typical distributions in particle size, namely, Gaussian distribution or normal distribution, log-normal distribution, and Rosin–Rammler distribution. These three size distribution functions are mostly used in the curve fitting of experimental data.

1.3.2.1 *Gaussian Distribution*

The Gaussian distribution, also known as the normal distribution, has the density function

$$f_N(d) = A_N \exp\left(-\frac{(d-d_0)^2}{2\sigma_d^2}\right) \tag{1.24}$$

where A_N is the normalizing constant; d_0 is the arithmetic mean of d; and σ_d is the standard deviation of d. Therefore, as given in Fig. 1.8, $2\sqrt{2}\sigma_d$ is the width of the distribution curve defined as the cord length of two points where

$$\frac{f_N(d)}{f_N(d_0)} = \frac{1}{e} \tag{1.25}$$

For a given sample, the particle size range is bounded by d_1 and d_2 as shown in Fig. 1.8. Thus, Eq. (1.16) becomes

$$\int_{d_1}^{d_2} A_N \exp\left(-\frac{(b-d_0)^2}{2\sigma_d^2}\right) db = 1 \tag{1.26}$$

from which A_N is obtained as

$$A_N = \frac{1}{\sigma_d}\sqrt{\frac{2}{\pi}}\left[\operatorname{erf}\left(\frac{d_2-d_0}{\sqrt{2}\sigma_d}\right) + \operatorname{erf}\left(\frac{d_0-d_1}{\sqrt{2}\sigma_d}\right)\right]^{-1} \tag{1.27}$$

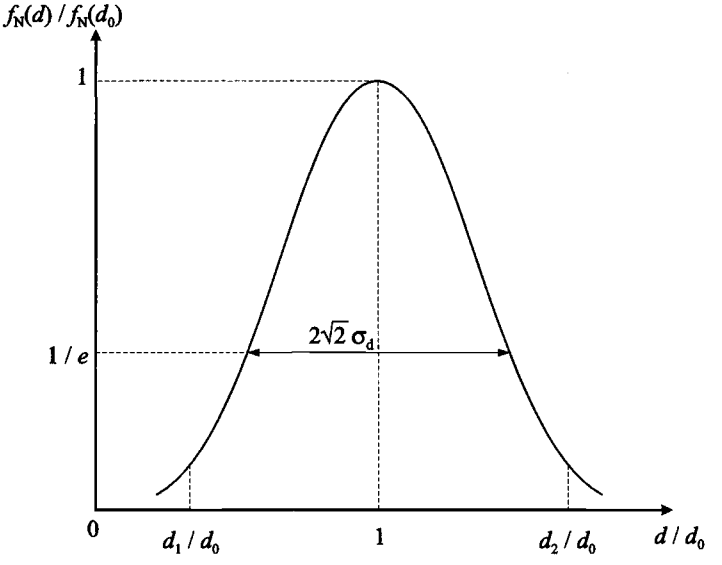

Figure 1.8. Gaussian distribution function.

Given the number density function of Eq. (1.24), the corresponding mass density function becomes

$$f_M(d) = A_M \frac{\pi}{6} \rho_p d^3 \exp\left(-\frac{(d-d_0)^2}{2\sigma_d^2}\right) \tag{1.28}$$

The normalizing constant A_M can be calculated from

$$\int_{d_1}^{d_2} A_M \frac{\pi}{6} \rho_p b^3 \exp\left(-\frac{(b-d_0)^2}{2\sigma_d^2}\right) db = 1 \tag{1.29}$$

There is no simple, exact, and explicit expression for A_M. However, for the case of a very narrow size distribution where $\sigma_d/d_0 \ll 1$, A_N and A_M are given by

$$A_N \approx \frac{1}{\sqrt{2\pi}\sigma_d} \tag{1.30}$$

and

$$\frac{1}{A_M} \approx \frac{(2\pi)^{3/2}}{6} \rho_p \frac{d_0}{\sigma_d}\left(\frac{3}{2} + \frac{d_0^2}{2\sigma_d^2}\right)\sigma_d^4 \tag{1.31}$$

For particle sizes following the Gaussian distribution described by Eqs. (1.24) and (1.30), 95 percent of the particles are of sizes between $(-2\sigma_d + d_0)$ and $(2\sigma_d + d_0)$.

1.3.2.2 *Log-Normal Distribution*

Most systems of fine particles have the log-normal type of particle size distribution. That is, with the logarithm of the particle size, the particle size distribution follows the normal or Gaussian distribution in semilog scales. Therefore, the density function for the log-normal distribution can be expressed by

$$f_N(d) = \frac{1}{\sqrt{2\pi}\sigma_{dl} d} \exp\left[-\frac{1}{2}\left(\frac{\ln d - \ln d_{0l}}{\sigma_{dl}}\right)^2\right] \tag{1.32a}$$

or

$$f_N(\ln d) = \frac{1}{\sqrt{2\pi}\sigma_{dl}} \exp\left[-\frac{1}{2}\left(\frac{\ln d - \ln d_{0l}}{\sigma_{dl}}\right)^2\right] \tag{1.32b}$$

Here, d_{0l} and σ_{dl} are parameters defining the log-normal distribution. d_{0l} is the median diameter, and σ_{dl} is the natural log of the ratio of the diameter for which the cumulative-distribution curve has the value of 0.841 to the median diameter. $\ln d_{0l}$ and σ_{dl} are not equivalent to the arithmetic mean and the standard deviation of $\ln d$, respectively, for the log-normal distribution (Problem 1.3). Note that, for the log-normal distribution, the particle number fraction in a size range of b to $b + db$ is expressed by $f_N(b)\,db$; alternatively, the particle number fraction in a parametric range of $\ln b$ to $\ln b + d(\ln b)$ is expressed by $f_N(\ln b)d(\ln b)$.

1.3.2.3 *Rosin–Rammler Distribution*

For broken coal, moon dust, and many irregular particles, the mass distribution is found to follow a form known as the Rosin–Rammler distribution. A Rosin–Rammler distribution has the density function

$$f_M(d) = \alpha\beta d^{\alpha-1} \exp(-\beta d^\alpha) \tag{1.33}$$

Table 1.5. α and β for Some Materials

Material	α	$\beta \times 10^3(\mu\text{m})^{-1}$
(a) Fine grinding		
Marlstone	0.675	33
Marlslate	0.839	33
Brown coal (lignite)	0.900	63
Feldspar	0.900	71
Cement clinker	1.000	29
Glass powder	1.111	25
Coal	1.192	21
(b) Coarse grinding		
Fullers clay	0.727	0.40
Coal, type 1	0.781	0.067
Coal, type 2	0.781	0.15
Limestone with 7% bitumen	0.781	0.13
Limestone, medium hardness	0.933	0.083
Limestone, hard	1.000	0.40
Clinker	1.036	0.50
Feldspar	1.111	0.50

Source: G. Herdan's *Small Particle Statistics*, Butterworths, London, 1960.

where α and β are constants. Integrating Eq. (1.33) yields the cumulative distribution function, F, as

$$F = \int_0^d f_M(b)\,db = 1 - \exp(-\beta d^\alpha) \tag{1.34}$$

However, the Rosin–Rammler distribution is often expressed in terms of R defined by

$$R = \int_d^\infty f_M(b)\,db = \exp(-\beta d^\alpha) \tag{1.35a}$$

Then, we have

$$\ln\left(\ln\frac{1}{R}\right) = \ln\beta + \alpha \ln d \tag{1.35b}$$

Equation (1.35b) shows that a linear relationship exists when $\ln[\ln(1/R)]$ is plotted against $\ln d$. From the slope and intercept of this straight line, α and β can be determined. α and β are typically obtained from the particle size distribution data based on sieve analyses. Table 1.5 provides a list of typical values of α and β for some materials for the Rosin–Rammler density function with d in the function having the unit micrometers (μm).

Example 1.2 A coarsely ground sample of corn kernel is analyzed for size distribution, as given in Table E1.3. Plot the density function curves for (1) normal or Gaussian distribution, (2) log-normal distribution, and (3) Rosin–Rammler distribution. Compare these distributions with the frequency distribution histogram based on the data and identify the distribution which best fits the data.

Table E1.3. *Data of Size Distribution*

Size range (mm)	Number of particles	Size range (mm)	Number of particles
0.05–0.10	1	0.50–0.55	3
0.10–0.15	5	0.55–0.60	1
0.15–0.20	6	0.60–0.65	2
0.20–0.25	7	0.65–0.70	0
0.25–0.30	8	0.70–0.75	1
0.30–0.35	6	0.75–0.80	0
0.35–0.40	4	0.80–0.85	1
0.40–0.45	4	0.85–0.90	0
0.45–0.50	4	0.90–0.95	1

Solution The data on numbers of particles in each particle range given in Table E1.3 can be converted to relative frequencies per unit of particle size as given in Table E1.4. The histogram for the relative frequency per unit of particle size for the data is plotted in Fig. E1.2; the histogram yields a total area of bars equal to unity. Superimposed on the histogram is the density function for the normal distribution based on Eqs. (1.24) and (1.30). For this distribution, the values for d_0 and σ_d are evaluated as 0.342 and 0.181, respectively. Also included in the figure is the density function for the log-normal distribution based on Eq. (1.32a). For this distribution, the values for $\ln d_{0l}$ and σ_{dl} are evaluated as -1.209 and 0.531, respectively.

Table E1.4. *Relative Frequency per Unit of Particle Size Data Given in Table E1.3*

Particle size (averaged, mm)	Number of particles	Relative frequency	Relative frequency per unit of particle size
0.075	1	0.019	0.370
0.125	5	0.093	1.852
0.175	6	0.111	2.222
0.225	7	0.130	2.593
0.275	8	0.148	2.963
0.325	6	0.111	2.222
0.375	4	0.074	1.481
0.425	4	0.074	1.481
0.475	4	0.074	1.481
0.525	3	0.056	1.111
0.575	1	0.019	0.370
0.625	2	0.037	0.741
0.675	0	0.000	0.000
0.725	1	0.019	0.370
0.775	0	0.000	0.000
0.825	1	0.019	0.370
0.875	0	0.000	0.000
0.925	1	0.019	0.370
Sum	54	1.000	20.00

For the Rosin–Rammler distribution, the distribution constants (α and β) are obtained from the particle mass distribution data. To obtain the mass density distribution, the data on

the number density distribution given in Table E1.3 need to be converted by using Eq. (1.23). From the converted data and with the least-square fitting based on Eq. (1.35b), α and β can be obtained as $\alpha = 3.71$ and $\beta = 4.88\ \text{mm}^{-1}$. Note that the unit for d in Eq. (1.33) would be millimeters when these α and β values are used. Thus, the mass density function of the Rosin–Rammler distribution can be calculated. Converting the mass density function to the number density function, the results for the Rosin–Rammler distribution are plotted as shown in Fig. E1.2.

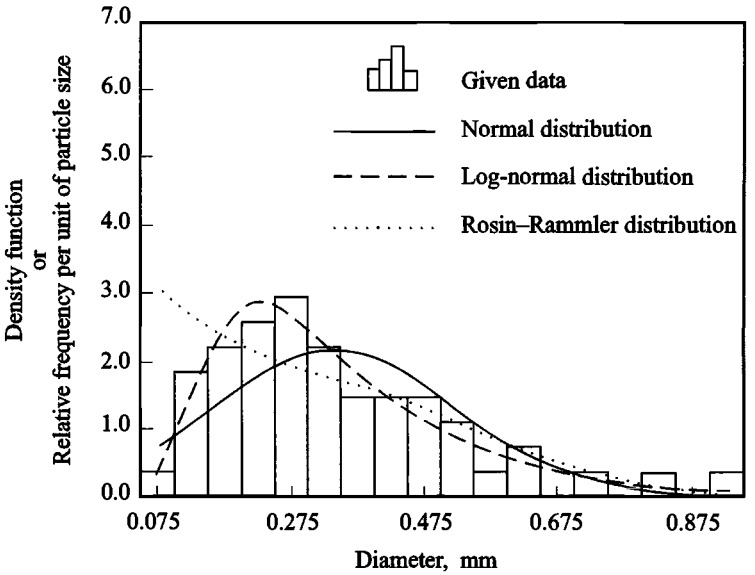

Figure E1.2. Comparisons of the relative frequency distribution based on the data with three density functions.

A graphical comparison of the three distributions with the given data shown in the figure reveals that the log-normal distribution best approximates the data.

1.3.3 *Averaged Diameters of a Particulate System*

For a given size distribution, various averaged diameters can be calculated, depending on the forms of weighing factors. The selection of an appropriate averaged diameter of a particle system depends on the specific needs of the application. For instance, in a pulverized coal combustion process, the surface area per unit volume may be important. In this case, Sauter's averaged diameter should be chosen.

1.3.3.1 *Arithmetic Mean Diameter*

The arithmetic mean diameter d_1 is the averaged diameter based on the number density function of the sample; d_1 is defined by

$$d_1 = \frac{\int_0^\infty b f_N(b)\, db}{\int_0^\infty f_N(b)\, db} \tag{1.36}$$

1.3.3.2 *Surface Mean Diameter*

The surface mean diameter d_S is the diameter of a hypothetical particle having the same averaged surface area as that of the given sample; d_S is given by

$$d_S^2 = \frac{\int_0^\infty b^2 f_N(b)\,db}{\int_0^\infty f_N(b)\,db} \tag{1.37}$$

1.3.3.3 *Volume Mean Diameter*

The volume mean diameter d_V is the diameter of a hypothetical particle having the same averaged volume as that of the given sample; d_V is determined by

$$d_V^3 = \frac{\int_0^\infty b^3 f_N(b)\,db}{\int_0^\infty f_N(b)\,db} \tag{1.38}$$

1.3.3.4 *Sauter's Mean Diameter*

Sauter's mean diameter d_{32} is the diameter of a hypothetical particle having the same averaged specific surface area per unit volume as that of the given sample; d_{32} is defined by

$$d_{32} = \frac{\int_0^\infty b^3 f_N(b)\,db}{\int_0^\infty b^2 f_N(b)\,db} \tag{1.39}$$

Note that Sauter's mean diameter in Eq. (1.39) is defined for a range of particle size, which is different from Sauter's diameter in Eq. (1.4), defined for a single particle size.

1.3.3.5 *DeBroucker's Mean Diameter*

DeBroucker's mean diameter d_{43} is the averaged diameter based on the mass density function of the sample; d_{43} is evaluated by

$$d_{43} = \frac{\int_0^\infty b^4 f_N(b)\,db}{\int_0^\infty b^3 f_N(b)\,db} = \frac{\int_0^\infty b f_M(b)\,db}{\int_0^\infty f_M(b)\,db} \tag{1.40}$$

1.4 Material Properties of Solids

The material properties of solids are affected by a number of complex factors. In a gas–solid flow, the particles are subjected to adsorption, electrification, various types of deformation (elastic, plastic, elastoplastic, or fracture), thermal conduction and radiation, and stresses induced by gas–solid interactions and solid-solid collisions. In addition, the particles may also be subjected to various field forces such as magnetic, electrostatic, and gravitational forces, as well as short-range forces such as van der Waals forces, which may affect the motion of particles.

In this section, we briefly discuss several aspects of the material properties of solids that are of interest to gas–solid flow applications. They include physical adsorption, deformation